12-2016

THSD1 (Thrombospondin Type 1 Domain Containing Protein 1) Mutation in the Pathogenesis of Intracranial Aneurysm and Subarachnoid Hemorrhage

Teresa Santiago-Sim

Xiaoqian Fang

Morgan L. Hennessy

Stephen V. Nalbach

Steven R. DePalma

See next page for additional authors

Authors

Teresa Santiago-Sim, Xiaoqian Fang, Morgan L. Hennessy, Stephen V. Nalbach, Steven R. DePalma, Ming Sum Lee, Steven C. Greenway, Barbara McDonough, and Georgene W. Hergenroeder

Published in final edited form as:

Stroke. 2016 December ; 47(12): 3005–3013. doi:10.1161/STROKEAHA.116.014161.

THSD1 Mutation in the Pathogenesis of Intracranial Aneurysm and Subarachnoid Hemorrhage

Teresa Santiago-Sim, Ph.D.[1], **Xiaoqian Fang, Ph.D.**[1], **Morgan L. Hennessy**[2], **Stephen V. Nalbach, M.D.**[2,3], **Steven R. DePalma, Ph.D.**[2], **Ming Sum Lee, M.D., Ph.D.**[4], **Steven C. Greenway, M.D.**[2], **Barbara McDonough, R.N**[2], **Georgene W. Hergenroeder, R.N., M.H.A.**[1], **Kyla J. Patek, M.S., C.G.C.**[1], **Sarah M. Colosimo, M.S., C.G.C.**[1], **Krista J. Qualmann, M.S., C.G.C.**[1], **John P. Hagan, Ph.D.**[1], **Dianna M. Milewicz, M.D., Ph.D.**[5], **Calum A. MacRae, M.D., Ph.D.**[4], **Susan M. Dymecki, M.D., Ph.D.**[2], **Christine E. Seidman, M.D.**[2,6,7], **J.G. Seidman, Ph.D.**[2], and **Dong H. Kim, M.D.**[1]

[1]Department of Neurosurgery, The University of Texas Medical School at Houston, Houston, TX 77030, U.S.A.

[2]Department of Genetics, Harvard Medical School, Boston, MA 02115, U.S.A.

[3]Department of Neurosurgery, Brigham and Women's Hospital, Boston, MA 02115, U.S.A.

[4]Department of Medicine, Brigham and Women's Hospital, Boston, MA 02115, U.S.A.

[5]Division of Medical Genetics, Department of Internal Medicine, The University of Texas Medical School at Houston, Houston, TX 77030, U.S.A.

[6]Cardiovascular Division, Brigham and Women's Hospital, Boston, MA 02115, U.S.A.

[7]Howard Hughes Medical Institute, Chevy Chase, MD 20815, U.S.A.

Abstract

Background and Purpose—A ruptured intracranial aneurysm (IA) is the leading cause of a subarachnoid hemorrhage (SAH). This study seeks to define a specific gene whose mutation leads to disease.

Methods—More than 500 IA probands and 100 affected families were enrolled and clinically characterized. Whole exome sequencing was performed on a large family, revealing a segregating THSD1 mutation. THSD1 was sequenced in other probands and controls. Thsd1 loss-of-function studies in zebrafish and mice were used for *in vivo* analyses, and functional studies performed using an *in vitro* endothelial cell model.

Results—A nonsense mutation in THSD1 (thrombospondin type-1 domain-containing protein 1) was identified that segregated with the 9 affected (3 suffered SAH; 6 had unruptured IA) and 13 unaffected family members (LOD score 4.69). Targeted THSD1 sequencing identified mutations in 8 of 507 unrelated IA probands, including 3 who had suffered SAH (1.6% [95% CI, 0.8%–

Correspondence to Dong H. Kim, M.D.: The University of Texas Medical School at Houston, 6431 Fannin Street, MSB 7.146, Houston, TX 77030, U.S.A. Tel: 713-500-6170; Fax: 713-500-0601; Dong.H.Kim@uth.tmc.edu.

Disclosures

None

3.1%]). These THSD1 mutations/rare variants were highly enriched in our IA patient cohort relative to 89,040 chromosomes in ExAC database ($p<0.0001$). In zebrafish and mice, Thsd1 loss-of-function caused cerebral bleeding (which localized to the subarachnoid space in mice) and increased mortality. Mechanistically, THSD1 loss impaired endothelial cell focal adhesion to the basement membrane. These adhesion defects could be rescued by expression of wild-type THSD1 but not THSD1 mutants identified in IA patients.

Conclusions—This report identifies THSD1 mutations in familial and sporadic IA patients, and shows that THSD1 loss results in cerebral bleeding in two animal models. This finding provides new insight into IA and SAH pathogenesis and provides new understanding of THSD1 function, which includes endothelial cell to extracellular matrix adhesion.

Keywords

Intracranial Aneurysm; Subarachnoid Hemorrhage; Medical Genetics; Animal Disease Models

INTRODUCTION

An intracranial aneurysm (IA) is a weakened area in a cerebral artery wall that leads to abnormal dilation and may rupture causing subarachnoid hemorrhage (SAH). The IA prevalence in the adult population is approximately 3%.[1] The overall annual incidence of SAH in developed countries is ~10 per 100,000.[2] In the United States alone, there are roughly 30,000 aneurysmal SAH cases per year.[2, 3] Despite treatment advances, the mortality of aneurysmal rupture is high and survivors experience high morbidity.[4–8] A family history, female gender, smoking, hypertension, and heavy alcohol consumption are significant risk factors for IA and/or SAH.[8, 9]

In a subset of patients, genetic factors play a role in IA pathogenesis. It is known that 7%–20% of patients have a positive family history and first-degree relatives are at increased risk, regardless of ethnic background.[10–16] Further, a genetic syndrome, Autosomal-Dominant Polycystic Kidney Disease (ADPKD), predisposes patients to IA formation (although the vast majority of familial and sporadic IA patients do not have ADPKD or other defined syndromes).[17] Nearly all cases of ADPKD are caused by mutations in either PDK1 or PDK2 that have a range of functions from forming a mechanosensor that regulates intracellular calcium levels to being involved in focal adhesions and the extracellular matrix.

In the majority of patients, IA formation is a sporadic disease without a family history. In addition, high-risk variants affecting a subset of families may be heterogeneous. For that reason, population-based approaches like genome-wide association studies have identified low-risk loci only.[18, 19] GWAS studies frequently miss rare variants with high disease impact.

Spontaneous SAH is often, but not always, caused by IA rupture.[20] The Nordic twin study showed that SAH has a heritability estimate of 41% (95% CI, 23.7%–55.5%); however, the vast majority of twins were discordant for SAH status.[21] The odds ratio for SAH is 51.0 (95% CI, 8.56–1117) when ≥2 affected first degree relatives have SAH.[22] Mackey and colleagues recently reported their study of 21 twin pairs where at least one was affected by

IA and both agreed to be study participants.[23] 11 of 12 monozygotic twins were both positive for IA, irrespective of differential risk factors (smoking history and hypertension), while only 5 of 9 dizygotic twins were both affected, suggesting that genetics plays a role in at least some IA cases.

In familial studies, linkage analyses of single IA families or sibling-pairs have mapped a number of susceptibility loci; however, no disease-causing IA mutation has been identified despite recent efforts, such as the multi-center Familial Intracranial Aneurysm Study.[24] Here, we report the identification of THSD1 mutations in both familial and sporadic IA cases and provide evidence using cell culture and animal models that THSD1 mutations contribute to disease.

METHODS

Expanded methods are provided in the supplement.

Study Participants

Starting in 2000, IA patients treated at The University of Texas at Houston or the Brigham and Women's Hospital had thorough phenotypic characterization and screening to identify affected family members. The Institutional Review Boards approved this study at both institutions and all study participants provided written informed consent. Over 500 IA probands and 100 affected families were enrolled and DNA samples obtained.

Those with a family history underwent genetic counseling, tracing of pedigrees with review of medical records, and screening of unaffected members using brain Magnetic Resonance Angiography (MRA). Only those subjects with IA documented by medical records or a positive result on MRA screening were designated as affected. All subjects with fusiform dilatations caused by atherosclerosis or acute dissection, arterial ectasia, fibromuscular dysplasia, other cerebrovascular abnormalities, and a defined or a suspected genetic condition (ADPKD) were excluded. We excluded one subject who developed IA following cranial radiation (which has been associated with increased incidence of IA).[25] In addition, we excluded subjects with small, possible aneurysms that were not validated on subsequent imaging.

All positive subjects had an aneurysmal dilatation in a normal artery with a risk for rupture. They were classified by anatomical shape as saccular or fusiform aneurysm (Fig. 1). Both were considered equivalent findings. For this study, we analyzed 35 family members from a European-American family (IA001), 507 unrelated IA patients and their families, and 305 controls with no known intracranial disease by medical history. We had information on rupture status for most of these patients. For those with known status, 52.2% had unruptured IA and 47.8% suffered SAH.

The control cohort was recruited at The University of Texas Medical School at Houston or the Brigham and Women's Hospital in Boston. No diagnostic tests were performed to exclude the presence of intracranial aneurysms in controls.

Detection of Mutations

Blood or saliva samples were collected from study participants and genomic DNA was extracted using standard methods or DNA purification kits (Flexigene or Oragene). In our previous study, linkage analysis in family IA001 identified an IA-susceptibility locus that maps to 13q14-21.[26] In the current study, we have characterized this family further using genome-wide whole exome-sequencing and copy number analysis.

Copy number analysis was performed on III-9 and IV-14 using the NimbleGen Human CGH 385K Whole-Genome Tiling microarray. Exome analysis was performed on IV-6 and IV-15 using the NimbleGen Sequence Capture 2.1 Exome Array and the Illumina Genome Analyzer. All coding exons and closely-flanking intronic regions in THSD1 (NM_018676) were sequenced in 507 IA probands and 305 controls via standard methods. Public data from the Exome Sequencing Project (ESP) and the Exome Aggregation Consortium (ExAC) were used to assess allelic frequency of identified variants.

Immunofluorescence and Histopathologic Analyses in Mice

Immunofluorescence and histopathologic analyses were performed on brain sections from the previously described Thsd1-Venus mouse strain.[27] Frozen brain sections were stained with 4′,6-diamidino-2-phenylindole (DAPI), anti-Venus, and anti-CD31 *or* anti-smooth muscle actin (SMA). Paraffin-embedded brain sections were stained with hematoxylin and eosin (H&E) stain.

Functional Analyses

Knockdown of the THSD1 ortholog in zebrafish, *LOC797520* (XM_001337954), was performed using a Morpholino Oligomer (MO) (5'-GCAAGCATGCATTCTTACCAAATCC-3') designed against the splice acceptor of exon 2. A MO from within the gene served as negative control (5'-AGACTTTCTGAGAAACTGGGCCTCT-3'). Different MO dosages were injected in zebrafish at the one-cell stage (n=53–70 per group). Images of live embryos at 48 hours post fertilization were obtained at 20× magnification using a Nikon TE2000 microscope. The Thsd1-Venus reporter knockin mice and their wild-type littermates were followed up to six months after birth. Brain magnetic resonance imaging (MRI) and angiography (MRA) were performed using a 9.4 Tesla Biospec 94/20 spectrometer.

THSD1 and negative control knockdown via transfection of siRNA (Stealth siRNA HSS148179 or Negative Control siRNA 12935-300, Life Technologies) was validated in cultured human umbilical vein endothelial cells (HUVEC) by Western and cell morphology was visualized by light microscopy. Effects on focal adhesion proteins (paxillin, phosphorylated focal adhesion kinase, and vinculin) were evaluated by immunofluorescence. Cell adhesion rescue experiments were performed on endogenous THSD1-depleted cells by siRNA co-transfection with the pCR3.1 vector carrying wild-type and mutant forms of THSD1 (L5F, R450X, R460W, E466G, G600E, P639L, T653I, and S775P) that were engineered to be siRNA-resistant by site-directed, silent mutagenesis (G993 and G996). THSD1 and talin interaction was assayed by co-immunoprecipitation.

Statistical Analysis

The chi-squared test with Yates' correction was used to compare the frequency of rare THSD1 loss-of-function variants in our 507 IA patient cohort between European cases and controls (http://graphpad.com/quickcalcs/contingency1.cfm). The 95% confidence interval for the proportion of IA and aneurysmal subarachnoid hemorrhage (SAH) in our cohort was calculated according to methods described by Robert Newcombe without a continuity correction (http://vassarstats.net/prop1.html).[28] The difference in frequency of intracranial hemorrhage between control MO and *LOC797520*-MO injected zebrafish was performed by chi-squared test. Differences in cerebral ventricular and whole brain volumes between the *Thsd1*-mutant and wild-type mouse groups were analyzed using the Welch Two Sample t-test. All *in vitro* experiments were performed in triplicates and repeated at least 3 times. Statistical data is presented as means with standard errors unless otherwise stated. The unpaired t-test was used for group comparisons.

RESULTS

IA001 Family

To identify an associated mutation, a large family with 9 members with IAs was characterized in detail (IA001; Fig. 1A and Supplemental Table I). The mean (± SD) age at IA diagnosis was 46.7 ± 12.2. The proband (III-9) presented with SAH and two other family members IV-15 and IV-17 also had SAH. Unruptured intracranial aneurysms (UIA) were determined by either medical history or MRA screening. Individuals were considered IA-negative after MRA screening. Two obligate carriers, III-3 and III-6, died of lung cancer and myocardial infarction at ages 77 and 69 years, respectively, without autopsies or MRA screens. Arterial dissections were present in two family members: a cervical carotid artery dissection (IV-6) and a coronary artery dissection (V-2). Smoking and hypertension data were available for 16 genotyped family members with known IA status (7 unaffected/9 affected). For the 7 family members without IA, 3, 2, 2, and 0 had a history of smoking, hypertension, both, or neither, respectively. For the 9 family members with IA, the numbers were 4, 2, 1, or 2. These modifiable risk factors in the IA001 family did not associate preferentially with IA versus non-IA status.

Although a dissection can precede the development of fusiform aneurysms,[20] these findings were not sufficient to be classified as positive. No clinical features associated with any other genetic syndrome were observed in the family.

Mutation Analyses

To define an associated mutation in the IA001 family, whole exome sequencing was performed on two affected family members (IV-6 and IV-15), identifying 53 heterozygous shared variants that alter protein sequences with minor allele frequencies (MAF) <0.1% in controls. Of particular interest, a nonsense mutation (R450X) was identified in thrombospondin type-1 domain-containing protein 1 (THSD1) gene (13:52952757, c.1348 C>T, NM_018676.3) that maps to 13q14.3. THSD1 (Fig. 1B) and encodes a transmembrane protein with a signal peptide (residues 1–24), extracellular domain (residues 25–413), and an intracellular domain (residues 435–852). The R450X mutation leads to a truncated protein

that lacks the intracellular domain. Segregation of R450X allele in all affected family members was noted (Fig. 1A) with a LOD score of 4.69 (disease frequency=0.032; penetrance=100%; R450X allele frequency=0.001). The variant was heterozygous in all affected persons, obligate carriers, and 3 members with unknown clinical status (III-12, IV-8, and V-2). This mutation was absent in unaffected relatives, our control cohort (n=305), and 89,040 chromosomes in the ExAC database. The R450X THSD1 variant co-segregates perfectly in all 22 cases with known IA status in the IA001 family. For 16 members of the IA001 family, we had data relative to smoking history and hypertension. All 7 unaffected members had a smoking history, hypertension or both. For the 9 affected members with IA, 7 of 9 had a smoking history, hypertension or both. Of note, two family members (IV-6 and V-2) that carried the R450X THSD1 mutation had arterial dissections, suggesting that THSD1 loss may be also be associated with dissections at low penetrance. No copy number variants were identified.

To interrogate the significance of THSD1 variants more broadly in IA, sequencing of all THSD1 coding exons and intron-exon boundaries was performed in 507 unrelated IA patients. Seven rare THSD1 heterozygous variants (<0.2% MAF in controls) were identified, all encoding missense residues: L5F in two probands, and R460W, E466G, G600E, P639L, T653I, and S775P in one proband each (Fig. 1B, Supplemental Table I). The proband carrying E466G had an affected daughter with the inherited variant. The other probands had sporadic disease. L5F, P639L, and S775P were absent in 89,040 control chromosomes from the ExAC database while R460W, E466G, G600E, and T653I were present in 2, 16, 45, and 6 control chromosomes, respectively (Supplemental Table II). These THSD1 mutations/rare variants were highly enriched in our IA patient cohort relative to 89,040 chromosomes in ExAC database ($p<0.0001$). Similarly, the 3 THSD1 mutations (R460W, E466G, and S775P) identified in known SAH individuals from our IA cohort were enriched relative to ExAC database ($p<0.0001$). L5F, R460W, E466G, G600E, and T653I are evolutionarily conserved amino acids (Fig. 1C) that are predicted by PolyPhen2 and SIFT to be functionally significant.

Thsd1 Expression in the Mammalian Brain

Since THSD1 variants are implicated in IA, we investigated the expression pattern of Thsd1 in the mammalian brain by utilizing a genetically engineered mouse model where the knockin of the fluorescent Venus reporter at the Thsd1 locus results in a Thsd1 knockout.[27] Thsd1-Venus expression co-localized with the endothelial cell marker, CD31, indicating endothelial-specific expression of Thsd1 in cerebral arteries (Fig. 2).

Loss of Thsd1 expression in zebrafish and mice disrupts the cerebrovasculature

To establish the role of *THSD1* in IA, two loss-of-function animal models were utilized. A zebrafish model was generated by embryonic injection of an antisense morpholino oligonucleotide at various concentrations that targets the splice acceptor site of exon 2 of the zebrafish *thsd1* ortholog (*LOC797520*). The loss of *thsd1* caused intracranial hemorrhages by 48 hours post fertilization in a dose-dependent manner (Fig. 3A), while embryos injected with control MO were unaffected (Fig. 3B). At each dose, the difference in hemorrhage rates

between control MO and *LOC797520* MO-injected zebrafish was significant (p<0.001). The majority of *thsd1*-morphant zebrafish did not survive to adulthood.

To interrogate the consequence of Thsd1 loss in mammals, we used the Thsd1 knockout mouse that contains a knockin of a fluorescent Venus reporter.[27] Thsd1$^{Venus/+}$ and Thsd1$^{Venus/Venus}$ mice survived to weaning age in expected Mendelian ratios. However, brain MRIs revealed mild to severe dilatation of cerebral ventricles consistent with hydrocephalus in a subset of mutant mice as young as 8 weeks (Fig. 4A). While total brain volumes in mutant mice [Thsd1$^{Venus/+}$ (*n=6*) and Thsd1$^{Venus/Venus}$ (*n=5*)] and wild-type mice [Thsd1$^{+/+}$ (*n=3*)] were similar between groups (mean±SD values in mm^3: 450.3±19.4 versus 431.0±13.8; p=0.17), ventricular volumes were significantly larger in the mutant group (11.7±4.7 in mutants; 6.7±0.3 in wild-types; p=0.005). Corresponding MRA imaging showed poor perfusion in mutant mice with the most marked hydrocephaly (Fig. 4A), suggesting increased intracranial pressure in these animals. No aneurysms were noted, and these scans were insufficiently sensitive to determine if SAH occurred in the mouse brains.

Among the 185 mutant and 74 wild-type mice in the colony, 5 heterozygotes died by 4 weeks (none of the wild-types). Gross examination at autopsy revealed massive cerebral bleeding in a SAH pattern (Fig. 4B). In addition, five mutant and three control mice were sacrificed for histological analysis at 16 weeks of age. Both subarachnoid hemorrhage and ventricular enlargement was noted in 1 of 2 Thsd1$^{Venus/+}$ and 1 of 3 Thsd1$^{Venus/Venus}$ mice but not wild-type littermates (n=3) (Fig. 4C).

Functional studies in HUVECs

A prior study in human lung fibroblasts suggested that THSD1 interacts with talin,[28] a key component of focal adhesions that mechanically link the intracellular actin bundles and integrin receptors that bind to the extracellular matrix. To test the hypothesis that THSD1 is involved in focal adhesions, THSD1 was analyzed in endothelial cells using loss-of-function and rescue experiments. Immunoblot confirmed THSD1 protein expression in cultured HUVECs and validated a THSD1-targeting siRNA (Fig. 5A). While cotransfection of treated cells with a vector containing siRNA-resistant wild-type THSD1 open reading frame restored THSD1 levels (Fig. 5A), the expression of the other mutants was variable. Notably, the L5F mutant in the signal peptide resulted in undetectable protein levels, implicating rapid mutant mRNA and/or protein turnover. In cells with the R450X construct, a truncated protein product was observed. Co-immunoprecipitation confirmed interaction of wild-type THSD1 and talin in HUVECs (Fig. 5B). Cell adhesion to fibronectin, collagen IV, or laminin was unchanged with THSD1 knockdown (data not shown), but adhesion to collagen I was significantly reduced (Fig. 5C). The cell adhesion defect was rescued by re-expression of wild-type THSD1 but not mutant THSD1 constructs. Compared to control cells, THSD1 siRNA-treated cells were significantly smaller with altered morphology and had fewer focal adhesions (Fig. 5D). THSD1 knockdown impacted the expression/localization of focal adhesion proteins paxillin, vinculin, and phosphorylated FAK (Y397). Altogether, these results suggest that THSD1 mutations perturb endothelial focal adhesions, cell morphology, and cell adhesion in ways that may contribute partially to IA.

DISCUSSION

We discovered in a large family a THSD1 truncating mutation (R450X) that segregated with disease. This mutation was present in all 9 affected cases (3 SAH and 6 UIA) and was absent in all 13 unaffected cases. In 8 unrelated probands, including those with sporadic disease, we identified THSD1 missense mutations that either exist in the signal peptide (L5F in two probands) or cluster in the intracellular region (R460W, E466G, G600E, P639L, T653I, and S775P). Overall, THSD1 mutations/rare variants that adversely affected protein function were found in 1.6% (95% CI, 0.8%–3.1%) and 1.9% (95% CI, 0.6%–5.3%) of total IA (507) and known SAH (162) cases, respectively, in our patient cohort. Therefore, other genetic and modifiable risk factors are primarily responsible for the vast majority of IA and SAH cases.

We analyzed two animal models to assess the consequence of Thsd1 loss. Thsd1$^{Venus/+}$ mice suffered increased mortality and cerebral hemorrhage localized to the subarachnoid space. Zebrafish develop intracranial hemorrhaging in a dose-dependent manner upon *thsd1* morpholino treatment. Recent work from Haasdijk and colleagues with a distinct *thsd1* morpholino has independently confirmed our zebrafish results.[29]

We did not observe IA formation in either model, although we can infer the presence of an aneurysm or other type of arterial weakening because of the hemorrhaging observed. It may be that our methods were inadequate to detect small aneurysms or that IA ruptured shortly after formation in these vertebrate model organisms. In human patients, it is known that small aneurysms, usually less than 3mm in size, cannot be adequately assessed by MRA.[30] The arteries in mice are significantly smaller than in human patients, and the aneurysms are likely to be smaller as well. Further, even histological sections cannot examine every part of the arteries, and therefore small aneurysms might have been missed. It is also possible that mice and zebrafish do not develop aneurysms at all, but exhibit arterial weakness in a different manner.

Our data show prominent Thsd1 expression in endothelial cells in murine cerebral arteries and highlight the significance of this protein in endothelial cell focal adhesion and attachment. THSD1 knockdown weakens endothelial cell-extracellular matrix binding as determined by cell culture studies. We also show that THSD1 interacts with talin. Of note, talin inactivation in endothelial cells had been shown to cause severe hemorrhaging in mouse embryos.[31] Taken together, these data suggest that talin and THSD1 interact to tether endothelial cells to the underlying basement membrane (see Supplemental Fig. 1 for a model). The cellular adhesion defects associated with THSD1 loss are rescued by the re-expression of wild-type THSD1 but not the mutant open reading frames identified in our IA subjects.

Other research supports the importance of endothelial cell function in IA pathogenesis; loss of endothelial specific expression of Sox17 promotes intracranial aneurysms in an elastase-treated hypertension mouse model.[32] Further, THSD1 shares some similarities to PDK1 and PDK2, two genes whose mutation causes Autosomal-Dominant Polycystic Kidney Disease (ADPKD) and increases IA risk.[17] In addition to a role as a mechanosensor, PDK1 and

PDK2 form a complex that is involved in focal adhesion and cell-extracellular matrix interactions.[33]

The significance of THSD1 mutations in other aneurysm types or more broadly in cardiovascular pathogenesis remains unclear. In our IA cohort, other types of clinical pathology were rare; however, in the IA001 family, two R450X patients had arterial dissections. It is possible that THSD1 defects are associated with acute dissections.

Overall, these results suggest that defects in THSD1 may lead to intracranial aneurysm formation and ultimately SAH, potentially via the disruption of endothelial cell adhesion to the extracellular matrix in cerebral arteries. These findings define several rare, high-risk genetic variants in THSD1 for IA and note a novel pathogenic pathway for a disease whose etiology had been poorly understood.[34]

Supplementary Material

Refer to Web version on PubMed Central for supplementary material.

Acknowledgments

We thank H. Nakauchi (University of Tokyo) for generously providing Thsd1 null mice and M. Lung (Hong Kong University of Science and Technology) for providing the pCR3.1 THSD1 expression vector. We are grateful to M. Farley and D. Bennett (Beth Israel Deaconess Medical Center) for technical support in magnetic resonance imaging.

Sources of Funding

This work was supported by the American Heart Association Bugher Foundation Award for Stroke Research, the US National Institutes of Health (National Institute of Neurological Disorders and Stroke, National Heart, Lung, and Blood Institute, and the National Center for Research Resources), the Vivian L. Smith Foundation for Neurologic Research, LeDucq Foundation, The Brain Aneurysm Foundation, and a Shared Instrumentation Grant S10RR028792 at Beth Israel Deaconess Medical Center (Boston, MA). The project described was also supported by award Number T32GM007753 from the National Institute of General Medical Sciences, an award T32HL007604 from the National Heart, Lung, and Blood Institute, and an R03NS087416 from the US National Institutes of Health. The content is solely the responsibility of the authors and does not necessarily represent the official views of the National Institute of General Medical Sciences or the National Institutes of Health.

References

1. Vlak MH, Algra A, Brandenburg R, Rinkel GJ. Prevalence of unruptured intracranial aneurysms, with emphasis on sex, age, comorbidity, country, and time period: A systematic review and meta-analysis. The Lancet. Neurology. 2011; 10:626–636. [PubMed: 21641282]
2. de Rooij NK, Linn FH, van der Plas JA, Algra A, Rinkel GJ. Incidence of subarachnoid haemorrhage: A systematic review with emphasis on region, age, gender and time trends. J Neurol Neurosurg Psychiatry. 2007; 78:1365–1372. [PubMed: 17470467]
3. King JT Jr. Epidemiology of aneurysmal subarachnoid hemorrhage. Neuroimaging clinics of North America. 1997; 7:659–668. [PubMed: 9336491]
4. Hop JW, Rinkel GJ, Algra A, van Gijn J. Case-fatality rates and functional outcome after subarachnoid hemorrhage: A systematic review. Stroke. 1997; 28:660–664. [PubMed: 9056628]
5. Tromp G, Weinsheimer S, Ronkainen A, Kuivaniemi H. Molecular basis and genetic predisposition to intracranial aneurysm. Annals of medicine. 2014; 46:597–606. [PubMed: 25117779]
6. Zacharia BE, Hickman ZL, Grobelny BT, DeRosa P, Kotchetkov I, Ducruet AF, et al. Epidemiology of aneurysmal subarachnoid hemorrhage. Neurosurgery clinics of North America. 2010; 21:221–233. [PubMed: 20380965]

7. Linn FH, Rinkel GJ, Algra A, van Gijn J. Incidence of subarachnoid hemorrhage: Role of region, year, and rate of computed tomography: A meta-analysis. Stroke. 1996; 27:625–629. [PubMed: 8614919]
8. Korja M, Silventoinen K, Laatikainen T, Jousilahti P, Salomaa V, Hernesniemi J, et al. Risk factors and their combined effects on the incidence rate of subarachnoid hemorrhage--a population-based cohort study. PLoS One. 2013; 8:e73760. [PubMed: 24040058]
9. Andreasen TH, Bartek J Jr, Andresen M, Springborg JB, Romner B. Modifiable risk factors for aneurysmal subarachnoid hemorrhage. Stroke. 2013; 44:3607–3612. [PubMed: 24193807]
10. Norrgard O, Angquist KA, Fodstad H, Forsell A, Lindberg M. Intracranial aneurysms and heredity. Neurosurgery. 1987; 20:236–239. [PubMed: 3561729]
11. Ronkainen A, Hernesniemi J, Ryynanen M. Familial subarachnoid hemorrhage in east Finland, 1977–1990. Neurosurgery. 1993; 33:787–796. discussion 796–797. [PubMed: 8264874]
12. Schievink WI, Schaid DJ, Michels VV, Piepgras DG. Familial aneurysmal subarachnoid hemorrhage: A community-based study. Journal of Neurosurgery. 1995; 83:426–429. [PubMed: 7666217]
13. Bromberg JE, Rinkel GJ, Algra A, Greebe P, van Duyn CM, Hasan D, et al. Subarachnoid haemorrhage in first and second degree relatives of patients with subarachnoid haemorrhage. BMJ. 1995; 311:288–289. [PubMed: 7633233]
14. Teasdale GM, Wardlaw JM, White PM, Murray G, Teasdale EM, Easton V. The familial risk of subarachnoid haemorrhage. Brain. 2005; 128:1677–1685. [PubMed: 15817512]
15. Ronkainen A, Hernesniemi J, Puranen M, Niemitukia L, Vanninen R, Ryynanen M, et al. Familial intracranial aneurysms. Lancet. 1997; 349:380–384. [PubMed: 9033463]
16. Kim DH, Van Ginhoven G, Milewicz DM. Incidence of familial intracranial aneurysms in 200 patients: Comparison among Caucasian, African-American, and Hispanic populations. Neurosurgery. 2003; 53:302–308. [PubMed: 12925244]
17. Drummond IA. Polycystins, focal adhesions and extracellular matrix interactions. Biochim Biophys Acta. 2011; 1812:1322–1326. [PubMed: 21396443]
18. Alg VS, Sofat R, Houlden H, Werring DJ. Genetic risk factors for intracranial aneurysms: A meta-analysis in more than 116,000 individuals. Neurology. 2013; 80:2154–2165. [PubMed: 23733552]
19. Hussain I, Duffis EJ, Gandhi CD, Prestigiacomo CJ. Genome-wide association studies of intracranial aneurysms: An update. Stroke. 2013; 44:2670–2675. [PubMed: 23908070]
20. Day AL, Gaposchkin CG, Yu CJ, Rivet DJ, Dacey RG Jr. Spontaneous fusiform middle cerebral artery aneurysms: Characteristics and a proposed mechanism of formation. Journal of Neurosurgery. 2003; 99:228–240. [PubMed: 12924694]
21. Korja M, Silventoinen K, McCarron P, Zdravkovic S, Skytthe A, Haapanen A, et al. Genetic epidemiology of spontaneous subarachnoid hemorrhage: Nordic twin study. Stroke. 2010; 41:2458–2462. [PubMed: 20847318]
22. Bor AS, Rinkel GJ, Adami J, Koffijberg H, Ekbom A, Buskens E, et al. Risk of subarachnoid haemorrhage according to number of affected relatives: A population based case-control study. Brain. 2008; 131:2662–2665. [PubMed: 18819992]
23. Mackey J, Brown RD, Sauerbeck L, Hornung R, Moomaw CJ, Koller DL, et al. Affected twins in the familial intracranial aneurysm study. Cerebrovasc Dis. 2015; 39:82–86. [PubMed: 25571891]
24. Foroud T, Lai D, Koller D, Van't Hof F, Kurki MI, Anderson CS, et al. Genome-wide association study of intracranial aneurysm identifies a new association on chromosome 7. Stroke. 2014; 45:3194–3199. [PubMed: 25256182]
25. Sciubba DM, Gallia GL, Recinos P, Garonzik IM, Clatterbuck RE. Intracranial aneurysm following radiation therapy during childhood for a brain tumor. Case report and review of the literature. Journal of Neurosurgery. 2006; 105:134–139. [PubMed: 16922075]
26. Santiago-Sim T, Depalma SR, Ju KL, McDonough B, Seidman CE, Seidman JG, et al. Genomewide linkage in a large Caucasian family maps a new locus for intracranial aneurysms to chromosome 13q. Stroke. 2009; 40:S57–S60. [PubMed: 19064780]
27. Takayanagi S, Hiroyama T, Yamazaki S, Nakajima T, Morita Y, Usui J, et al. Genetic marking of hematopoietic stem and endothelial cells: Identification of the Tmtsp gene encoding a novel cell

surface protein with the thrombospondin-1 domain. Blood. 2006; 107:4317–4325. [PubMed: 16455951]

28. de Hoog CL, Foster LJ, Mann M. RNA and RNA binding proteins participate in early stages of cell spreading through spreading initiation centers. Cell. 2004; 117:649–662. [PubMed: 15163412]
29. Haasdijk RA, Den Dekker WK, Cheng C, Tempel D, Szulcek R, Bos FL, et al. THSD1 preserves vascular integrity and protects against intraplaque haemorrhaging in ApoE−/− mice. Cardiovasc Res. 2016; 110:129–139. [PubMed: 26822228]
30. Schwab KE, Gailloud P, Wyse G, Tamargo RJ. Limitations of magnetic resonance imaging and magnetic resonance angiography in the diagnosis of intracranial aneurysms. Neurosurgery. 2008; 63:29–34. discussion 34-25. [PubMed: 18728566]
31. Monkley SJ, Kostourou V, Spence L, Petrich B, Coleman S, Ginsberg MH, et al. Endothelial cell talin1 is essential for embryonic angiogenesis. Dev Biol. 2011; 349:494–502. [PubMed: 21081121]
32. Lee S, Kim IK, Ahn JS, Woo DC, Kim ST, Song S, et al. Deficiency of endothelium-specific transcription factor Sox17 induces intracranial aneurysm. Circulation. 2015; 131:995–1005. [PubMed: 25596186]
33. Hassane S, Claij N, Lantinga-van Leeuwen IS, Van Munsteren JC, Van Lent N, Hanemaaijer R, et al. Pathogenic sequence for dissecting aneurysm formation in a hypomorphic polycystic kidney disease 1 mouse model. Arterioscler Thromb Vasc Biol. 2007; 27:2177–2183. [PubMed: 17656674]
34. Santiago-Sim, T., Kim, DH. Pathobiology of intracranial aneurysms. In: W, HR., editor. Youmans Neurological Surgery 6e. Philadelphia, PA: Elsevior Saunders; 2011. p. 3747-3755.

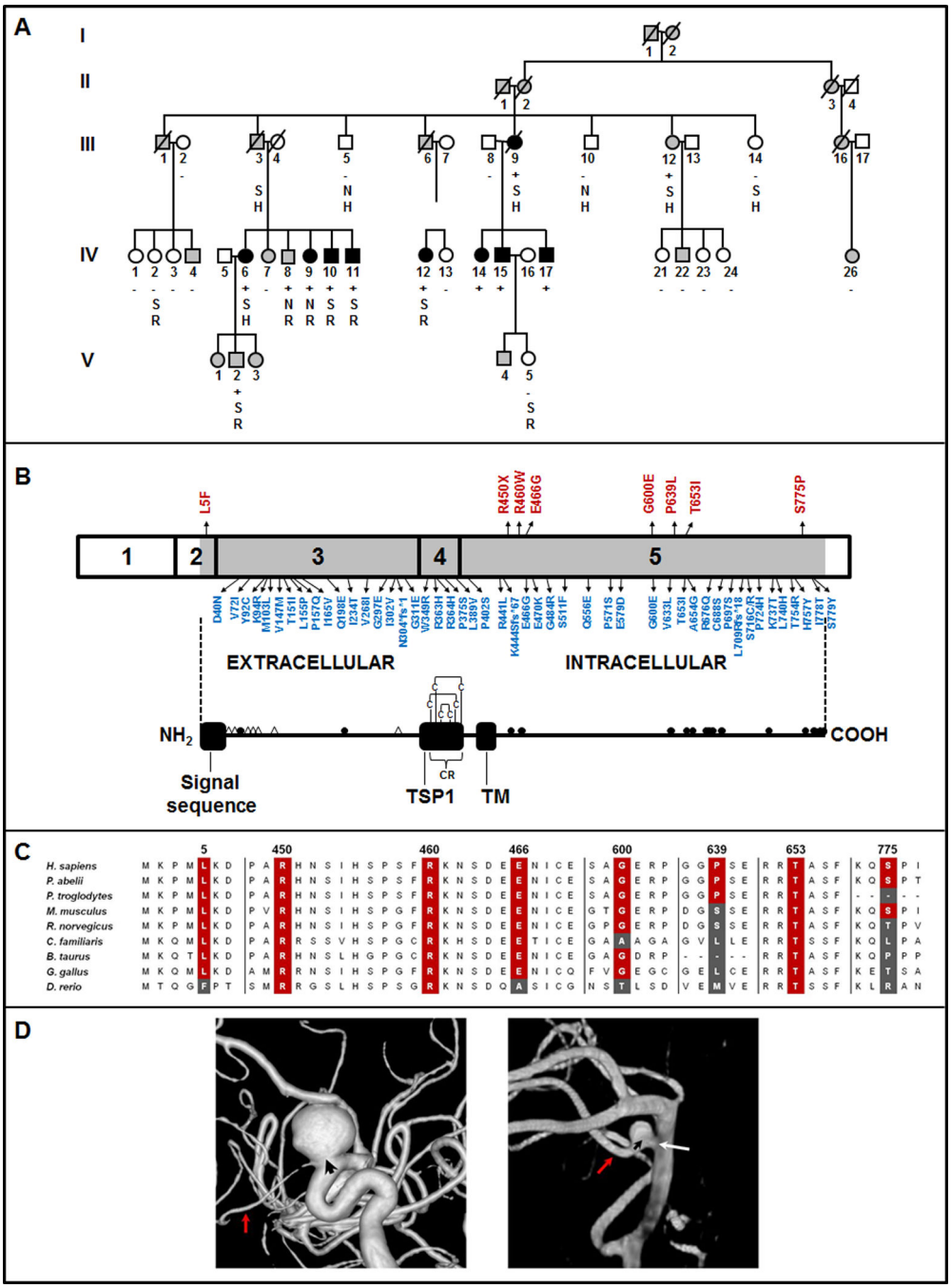

Figure 1. Identification of the THSD1 R450X mutation in a large family with IA and the spectrum of THSD1 rare variants

A, Pedigree of family IA001. Squares represent males, circles females, black symbols affected persons, white symbols unaffected persons, gray symbols unknown phenotype, “+” and “−” symbols denote R450X mutation carriers and non-carriers, respectively, as identified by sequencing. Slashes denote deceased individuals. Of the 9 affected individuals, 3 had SAH (III-9, IV-15, and IV-17) while the rest had UIA. **B**, THSD1 rare variants in unrelated IA patients (red) and in control individuals (blue) in relation to numbered exons

and protein domains. THSD1 control variants are from the NHLBI GO Exome Sequencing Project. TSP1 denotes thrombospondin type 1 repeat, CR cysteine-rich region, TM transmembrane domain, triangles predicted N-glycosylation sites, and circles predicted phosphorylation sites. **C**, THSD1 alignments highlight evolutionary conservation of substituted amino acids. **D**, Aneurysm images in patients with THSD1 variants. On the left, a digital subtraction angiogram shows a 9-mm right ophthalmic artery saccular aneurysm in subject III-9 of family IA001 with the R450X mutation. This aneurysm is termed saccular because the neck (black arrow) arises from an arterial branch point, the internal carotid artery (at the base of the aneurysm neck) and the opthalmic artery (red arrow). On the right, a magnetic resonance angiogram shows a 3-mm right superior cerebellar artery aneurysm in patient NR0756 with sporadic disease and with the P639L variant. This aneurysm is defined as fusiform, since it arises from the trunk of the superior cerebellar artery (red arrow). The white arrow indicates the branch point between the basilar artery and the superior cerebellar artery. The aneurysm neck (black arrow) arises just distal to this branch point. Both represent weakened areas of the arterial wall that can rupture.

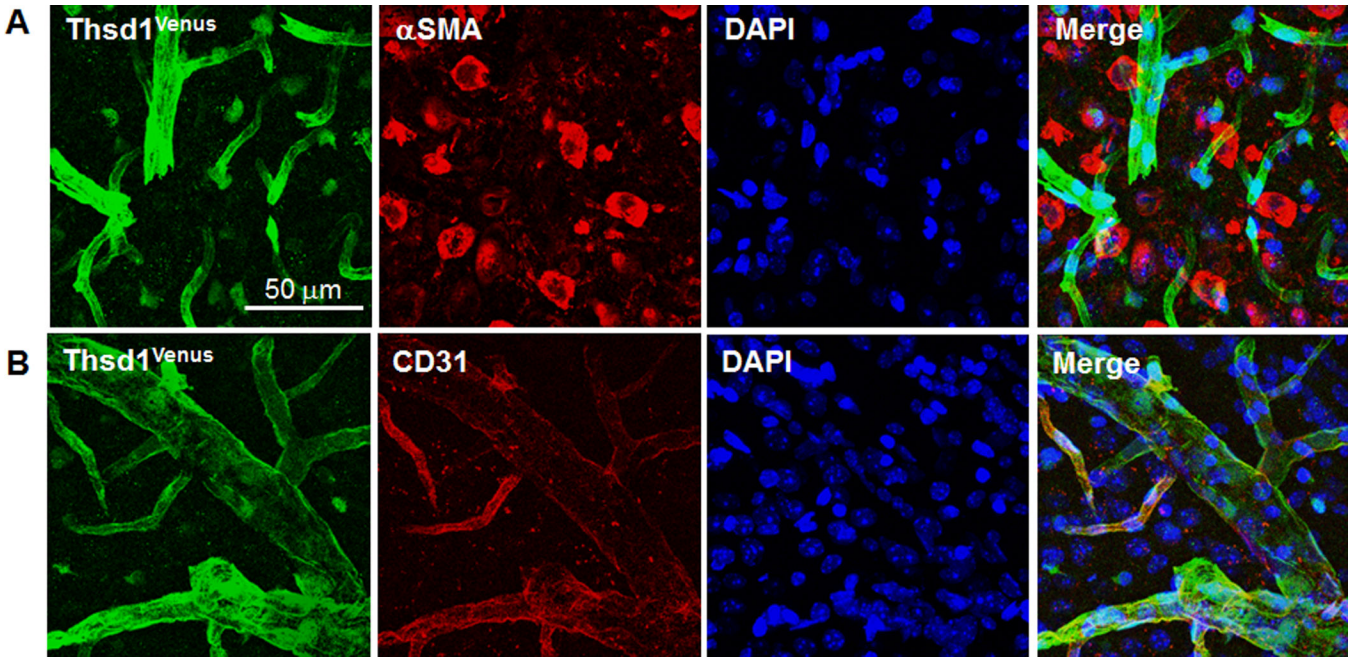

Figure 2. Thsd1 is expressed in the vascular endothelium but not smooth muscle in mouse brains

A, and **B**, Thsd1 *Venus* fluorescence (far left) consistently colocalized with the endothelial marker CD31 (bottom) but not with alpha smooth muscle actin (αSMA), a marker for smooth muscle cells (top). Nuclei were DAPI stained.

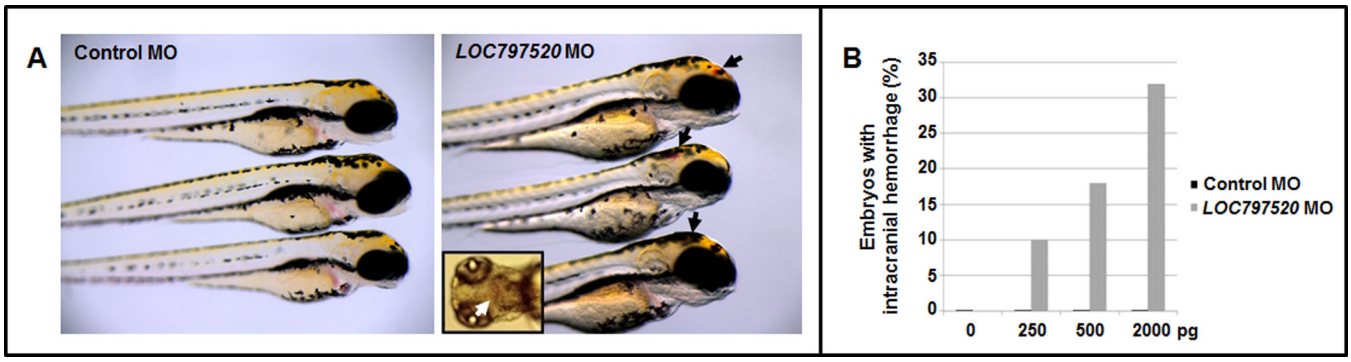

Figure 3. Loss of *thsd1* in zebrafish impairs the cerebrovasculature

A, zebrafish embryos at 48 hours post-fertilization injected with control or *LOC797520* (*thsd1*) Morpholino Oligonucleotides (MO) at the one-cell stage. Inset shows dorsal view of a *thsd1* morphant embryo. **B**, Quantification of zebrafish embryos with intracranial hemorrhage at 48 hours post-fertilization treated with various doses of control or *LOC797520* MO. For each MO injection, 53–70 embryos were analyzed per group and the difference in frequency of hemorrhage between control MO and *LOC797520* MO-injected embryos was significant ($p<0.001$).

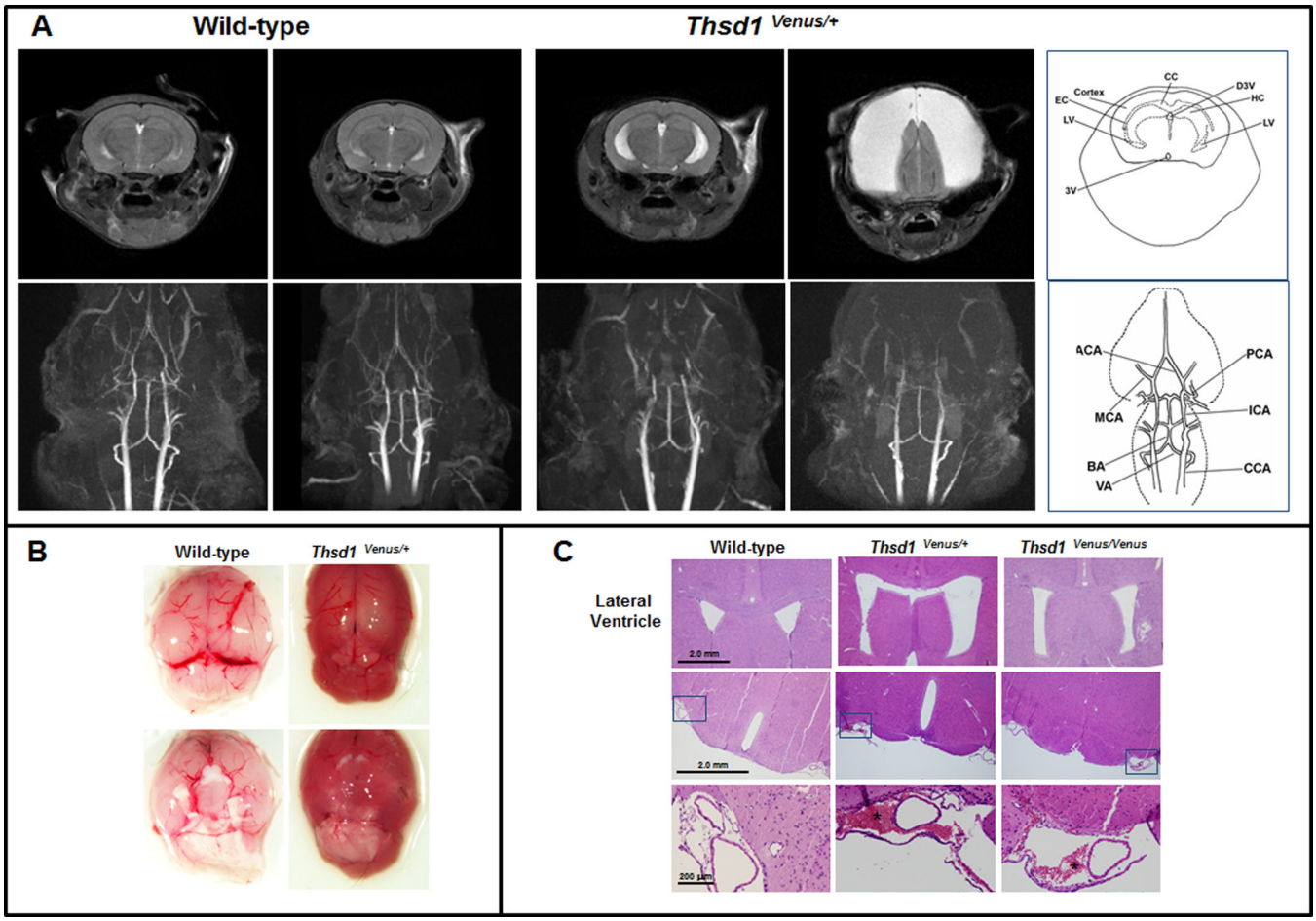

Figure 4. Loss of Thsd1 expression in mice disrupts the cerebrovasculature

A, coronal T2-weighted brain MRIs and corresponding MRA images of cerebral vessels of 8-week old wild-type and Thsd1 $^{Venus/+}$ mice. MRI analysis showed mild to severe dilatation of cerebral ventricles in a subset of Thsd1-mutant mice. MRA images showed poor visualization of blood flow in mice with severe ventricular dilatation. In wild-type animals, no ventricular dilatation was observed, and the vessels of the circle of Willis and emerging small vessels were well-delineated. The right panel shows schematic diagrams of normal brain regions and cerebral arteries. 3V, 3rd ventricle; LV, lateral ventricle; EC, external capsule; CC, corpus callosum; D3V, dorsal 3rd ventricle; HC, hippocampus; VA, vertebral artery; BA, basilar artery; MCA, middle cerebral artery; ACA, anterior cerebral artery; PCA, posterior cerebral artery; ICA, internal carotid artery; CCA, common carotid artery. **B**, the brain of a Thsd1 $^{Venus/+}$ mouse that died suddenly at 9 weeks and that of a wild-type mouse sacrificed at 9 weeks. Both brains were from non-perfused animals and imaged under the same dissecting microscope. Unlike the wild-type brain, the Thsd1 $^{Venus/+}$ brain showed massive and diffuse cerebral hemorrhage. **C**, H&E staining of brain slices from wild-type, Thsd1 $^{Venus/+}$ and Thsd1 $^{Venu/Venus}$ show enlargement of lateral ventricles and extravasation of blood into the subarachnoid space (*) in a subset of mutant animals. No bleeding occurred in wild-type mice.

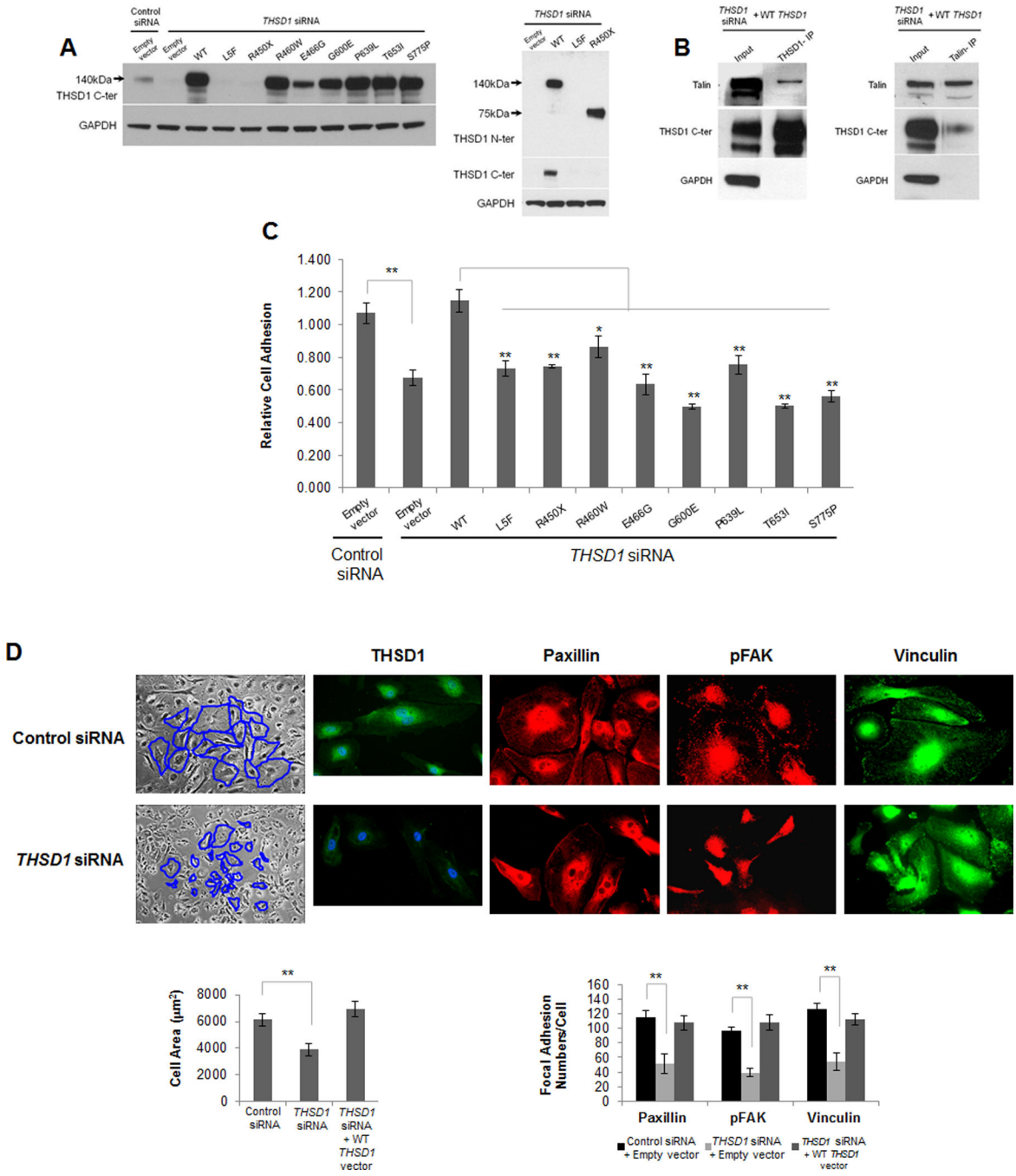

Figure 5. Functional analyses of THSD1 in HUVECs

A) Transfection of HUVECs with targeting siRNA inhibited THSD1 relative to control siRNA-treated cells as determined by Western. The THSD1 open reading frame in pCR3.1 was engineered by silent mutagenesis to be siRNA-resistant and was used as a template for both WT and mutant THSD1 constructs. Co-transfection of THSD1 siRNA and the vector expressing wild-type THSD1 restored expression. In contrast, the L5F mutant resulted in undetectable protein expression, while R450X led to a truncated protein. C-terminal (C-ter) and N-terminal (N-ter)-targeting THSD1 antibodies. **B)** THSD1 and talin co-

immunoprecipitate each other in HUVEC cells. Cell lysates of HUVECs transfected with WT THSD1 vector were subjected to immunoprecipitation (IP) with either an anti-C-ter THSD1 antibody (left panel) or anti-talin antibody (right panel) and immunoblotted with anti-talin, anti-C-ter THSD1 or anti-GAPDH antibody. **C)** Cell adhesion defects to collagen I in THSD1 siRNA-treated cells are rescued by co-transfection of siRNA-resistant wild-type but not variant THSD1 from IA-patients. * and ** denotes $P<0.05$ and $P<0.001$, respectively. **D)** (top) light microscopy imaging and immunofluorescence analyses of cells treated with a control or THSD1 siRNA; (bottom) quantification for cell areas (left) and focal adhesion numbers (right). Cell peripheries are shown in blue. In immunofluorescence staining, cells were stained with anti-C-ter THSD1, anti-paxillin, anti-pFAK (Y397) and anti-vinculin antibodies. A significant reduction in cell size and focal adhesion number was observed in THSD1 siRNA-treated cells.